C-Terminal Domains of Na^+/H^+ Exchanger Isoform 3 Are Involved in the Basal and Serum-Stimulated Membrane Trafficking of the Exchanger†

Shafinaz Akhter, Megan E. Cavet, Chung-Ming Tse, and Mark Donowitz*

Division of Gastroenterology, Department of Medicine, Johns Hopkins University School of Medicine, Baltimore, Maryland 21205

Received July 27, 1999; Revised Manuscript Received November 2, 1999

ABSTRACT: When expressed either in polarized epithelial cells or in fibroblasts, two Na^+/H^+ exchanger isoforms, NHE1 and NHE3, have different subcellular distributions. Using a quantitative cell surface biotinylation technique, we found PS120 cells target ∼90% of mature NHE1 but only 14% of NHE3 to the cell surface, and this pattern occurs irrespective of NHE protein expression levels. In this study, we examined surface fractions of NHE3 C-terminal truncation mutants to identify domains involved in the targeting of NHE3. Removing the C-terminal 76 amino acids doubled surface fractions to 30% of total and doubled the V_{max} from 1300 to 2432 μM H^+/s. Removal of another 66 amino acids increased surface levels to 55% of total with an increase in the V_{max} to 5794 μM H^+/s. Surface fractions did not change with a further 105 amino acid truncation. We postulated that inhibition of the basal recycling of NHE3 could result in the surface accumulation of the NHE3 truncations. Accordingly, we found that, unlike wild-type NHE3, the truncations were shown to internalize poorly and were not affected by PI3 kinase inhibition. However, while the truncations demonstrated reduced basal recycling, they retained the same serum response as full-length NHE3, with a mobilization of ∼10% of total NHE to the surface. We conclude that basal recycling of NHE3 is controlled by endocytic determinants contained within its C-terminal 142 amino acids and that serum-mediated exocytosis is independently regulated through a different part of the protein.

Na^+/H^+ exchangers (NHEs)[1] are a family of integral membrane proteins that mediate the electroneutral exchange of Na^+ for H^+. The six cloned NHEs, named NHE1−NHE6 according to the order of their discovery, demonstrate differences in their mechanism of regulation as well as their expression patterns. Each NHE is composed of 10−12 transmembrane domains in its N-terminus that mediate the movement of Na^+ and H^+ across the plasma membrane and a long cytoplasmic C-terminal tail that allows the regulation of the transport function. Na^+/H^+ exchangers demonstrate 50−60% amino acid identity in their N-terminal transport domains. In contrast, NHE isoforms demonstrate <25% amino acid identity in their C-terminal domains, which determine the unique characteristics of the regulation of an individual NHE (for reviews see refs *1* and *2*).

Among the members of the cloned Na^+/H^+ exchanger gene family, NHE1 and NHE3 are the best-characterized isoforms. NHE1 is the ubiquitously expressed isoform and in epithelial cells is found on the basolateral membrane, where it mediates such "housekeeping" functions as maintaining intracellular pH homeostasis, modulating cell volume (*3*), and perhaps helping organize the actin cytoskeleton (*4*). Both transfected and endogenous mature NHE1 in polarized and unpolarized cells demonstrates a largely plasma membrane localization, which does not appear to change as a part of regulation (*5*−*7*). The acute regulation of NHE1 by growth factors and protein kinases occurs through changes in its affinity for intracellular H^+ ($K'[H^+]_i$). The mechanism of NHE1 regulation is through changes in the activity of individual molecules and is mediated by phosphorylation-dependent and independent modifications of two critical domains in its cytoplasmic portion (*8*−*10*).

NHE3 has a much more limited expression pattern and is found predominantly on the brush border membrane of small intestine, colon, gall bladder, kidney proximal tubule and thick ascending loop of Henle, and salivary gland ducts, where it is involved in transcellular Na^+ absorption. We have previously shown that the regulation of NHE3, unlike NHE1, is through multiple separate subdomains found throughout its cytoplasmic portion, which act to set the basal V_{max} as well as to alter the V_{max} under regulated conditions. In addition, we found that truncation of the C-terminal 76 amino acids increased the rate of basal NHE3 activity, although the mechanism of this effect was not elucidated beyond the suggestion that these amino acids served an inhibitory function (*11*).

† These studies were supported by National Institute of Diabetes and Digestive and Kidney Diseases Grants RO1-DK-26523, PO1-DK-44484, and DK-51116, the Meyerhoff Digestive Diseases Center, and the Hopkins Center for Epithelial Disorders. M.E.C. was supported by a Wellcome International Travelling Fellowship, United Kingdom.

* Correspondence should be addressed to this author at The Johns Hopkins University School of Medicine, 918 Ross Research Bldg, 720 Rutland Ave., Baltimore, MD 21205-2195. Phone (410) 955-9675; Fax: (410) 955-9677; E-mail mdonowit@welch.jhu.edu.

[1] Abbreviations: NHE, Na^+/H^+ exchanger; OK cells, opossum kidney cells; SDS−PAGE, sodium dodecyl sulfate−polyacrylamide gel electrophesis; ECL, enhanced chemiluminescence; PTH, parathyroid hormone; EGF, epidermal growth factor; FBS, fetal bovine serum.

10.1021/bi991739s CCC: $19.00
Published on Web 02/02/2000

The mechanism of NHE3 regulation is through changes in the maximal activity of individual exchangers and/or in the total amount of active NHE3 on the plasma membrane. The role of membrane trafficking in NHE3 regulation has been suggested with the observations that endogenous NHE3 in kidney cortex (*12*), intestinal Caco-2 cells (*13*), and opossum kidney (OK) cells (*14*, *15*) is found both on the brush border membrane as well as in a subapical compartment. Furthermore, NHE3 has been shown to move between these two locations in response to various signaling pathways as part of the regulation of NHE3 activity (*13*, *14*−*17*).

This aspect of endogenous NHE3 is reproduced when the protein is exogenously expressed in two independent Na^+/H^+ exchanger-deficient fibroblast cell lines, PS120 and AP1. Recent studies in PS120 and AP1 cells have demonstrated that only a small fraction of NHE3 is found on the plasma membrane under basal conditions (*18*, *19*). In fact, the majority of the exchanger is present within an intracellular juxtanuclear compartment. While not definitively identified, studies showing that a population of intracellular NHE3 colocalizes with both the transferrin receptor and cellubrevin suggested that the intracellular compartment of NHE3 is recycling endosomes, from which it is postulated that NHE3 traffics to and from the plasma membrane. Thus, a role for endo/exocytosis in both the basal and regulated activity of NHE3 appears likely (*19*).

To quantitatively examine the role of membrane trafficking in basal and regulated NHE1 and NHE3 activity, as well as to identify domains within NHE3 involved in these processes, the plasma membrane expression of both exchangers had to be determined. Consequently, we developed a method using cell surface biotinylation that allowed us to quantitate the plasma membrane fractions of NHE protein. This method was used to quantitate the plasma membrane fractions of full-length NHE1 and NHE3, as well as C-terminal truncation mutants of NHE3, under both basal and serum-stimulated conditions. We have previously reported that the 377 C-terminal amino acids of NHE3 comprise the domain necessary for all basal and regulated modulation of NHE3 activity, with serum acting through the very N-terminal 19 amino acids of this domain (*11*). We now report that a subdomain of this region, the C-terminal 142 amino acids, reduces basal plasma membrane expression of NHE3 by mediating the endocytosis of the exchanger. Furthermore, we found that basal and serum-stimulated membrane trafficking of NHE3 are independently regulated and act through different domains in the C-terminus of the exchanger.

EXPERIMENTAL PROCEDURES

DNA Constructs. NHE3V truncation mutants were generated from NHE3 tagged at the C-terminus with the vesicular stomatitus virus G protein (VSV-G) epitope and linker sequence. A convenient *Xho*I restriction site at the junction between NHE3 and the VSV-G sequence allowed the design of antisense primers with the internal sequence at the desired sites of truncation and an *Xho*I site inserted at the 5′ end. Fragments were generated by PCR with upsteam sense primers with convenient restriction sites and the internal antisense primers with the engineered *Xho*I sites. Fragments were then ligated into the NHE3V plasmid and cut with *Xho*I and the upstream restriction enzyme, and their sequence was verified by both restriction analysis and sequencing of junctions.

The double leucine deletion mutants were constructed by use of a set of complementary primers of the surrounding sequences with the six base pairs deleted. Fragments were generated by PCR with the mutated primers and convenient upstream and downstream primers and then ligated together by PCR with the flanking primers.

Cell Culture. Chinese hamster ovary (CHO) cell-derived PS120 fibroblasts were stably transfected with cDNAs for full-length rabbit NHE3V, E3/756V, E3/690V, and E3/585V and human NHE1V, using the lipofectamine reagent (Life Technologies). They were grown in Dulbecco's modified Eagle's medium (DMEM) supplemented with 25 mM $NaHCO_3$, 10 mM HEPES, 50 units/mL penicillin, 50 μg/mL streptomycin, and 10% fetal bovine serum in a 5% CO_2/95% O_2 incubator at 37 °C, as described (*20*). G418 (400 μg/mL) was used to maintain selection pressure and was added immediately after each subculturing. In addition, cells were exposed to an acid load consisting of 50 mM NH_4Cl/saline solution for 1 h, followed by an isotonic 2 mM Na^+ solution. Surviving cells were then placed in normal culture medium and allowed to reach 30−50% confluence. The acidification process was initially repeated every 2−3 days until more than 50% of the cells survived and was then repeated every week to maintain high Na^+/H^+ exchange activity.

Crude Membrane Preparation. Transfected PS120 cells were grown to confluence in 10-cm Petri dishes. All subsequent manipulations of the cells were conducted at 4 °C with ice-cold solutions. The cells were washed three times with PBS and once with 5 mM sodium phosphate, pH 8, with protease inhibitors. The cells were scraped in 1−2 mL of 5 mM sodium phosphate, sonicated briefly, and centrifuged at 3000*g* for 10 min to spin down nuclei and unbroken cells. The resulting supernatant was centrifuged at 30000*g* for 30 min to pellet the cell membranes, and the pellet was homogenized by passing through a 26 $^1/_8$ gauge needle in 100−300 μL of sodium phosphate buffer.

Cell Surface Biotinylation. Transfected PS120 cells were grown to 70−80% confluence in 10-cm Petri dishes. The cells were then serum-starved for 5 h. For serum conditions, 10% dialyzed FBS was supplemented for 15 min at 37 °C, and for wortmannin conditions, 100 nM wortmannin was supplemented for 60 min at 37 °C. All subsequent manipulations were performed at 4 °C. Cells were washed twice in phosphate-buffered saline (150 mM NaCl and 20 mM Na_2HPO_4, pH 7.4) and once in borate buffer (154 mM NaCl, 10 mM boric acid, 7.2 mM KCl, and 1.8 mM $CaCl_2$, pH 9). The surface plasma membrane proteins were then biotinylated by gently shaking the cells for 20 min with 3 mL of borate buffer containing 1.5 mg of NHS−SS−biotin (biotinylation solution; Pierce). An additional 3 mL of the same biotinylation solution was then added, and the cells were rocked for an additional 20 min. The biotinylation solution was then discarded, and the cells were washed extensively with the quenching buffer (20 mM Tris and 120 mM NaCl, pH 7.4) to scavenge the unreacted biotin, and then the cells were washed twice with phosphate-buffered saline.

Cells were then scraped and solubilized with 1 mL of N^+ buffer (60 mM HEPES, pH 7.4, 150 mM NaCl, 3 mM KCl, 5 mM Na_3EDTA, 3 mM EGTA, and 1% Triton X-100) and

were then sonicated for 20 s and agitated on a rotating rocker at 4 °C for 30 min, followed by centrifugation at 12000*g* for 30 min to remove insoluble cellular debris.

A portion of the resulting supernatant was retained as the total fraction. The remaining total was then incubated with avidin−agarose (Pierce) for 2 h to separate the biotinylated proteins from nonbiotinylated proteins by binding the former to avidin-agarose. After two consecutive avidin precipations, the remaining supernatant was retained as the intracellular fraction. Finally, the avidin−agarose beads were washed repeatedly in N^+ buffer to remove all the nonspecifically bound proteins, and the bound proteins were solubilized in equivalent volumes (to volume initially added to beads) of sample buffer containing β-mercaptoethanol to cleave the disulfide bonds of the NHS−SS−biotin and then heated gently at 70 °C for 5 min, yielding the surface fraction. Three dilutions of the total, intracellular, and surface fractions were run on the same 9% polyacrylamide gel and transferred to Immobilon membranes. Western analysis was performed with monoclonal anti-VSV-G antibody (P5D4 hybridoma supernatant) as the primary antibody and horseradish peroxidase-conjugated anti-mouse as the secondary antibody. Bands were then visualized for enhanced chemiluminescence (ECL) on preflashed film under developing conditions in which the dilutions gave linear signals.

Quantitation of Fractions. The volume of each band was determined in arbitrary densitometric units by use of a scanning densitometer and Imagequant software. Values for each band were plotted as densitometric units versus sample volume. Curves for each fraction (total, intracellular, and surface) were generated and analyzed by linear analysis on Origin software. Fractions were quantitated as the percentage of total as follows: (1) the sample volume needed to give the same densitometric value was determined for each fractions present; (2) the sample volumes for each fraction were compared against the volume of the total fraction needed to give the same densitometric value only when they fell on the linear range of all curves simultaneously; and (3) values were used only if recovery (i.e., surface plus intracellular) equaled or exceeded 85% of total NHE3.

Reversible Biotinylation. The protocol described above was modified to determine the amount of internalized NHE3. Cells were biotinylated as described above at 4 °C; they were then incubated at 37 °C for the indicated times in the presence or absence of wortmannin (100 nM). Cells were then returned to 4 °C, when all remaining surface biotin was removed by addition of 10 mM freshly added 2-mercaptoethanesulfonic acid (MESNA) for 3 × 30 min washes in stripping buffer (100 mM NaCl, 1mM EDTA, 50 mM Tris, pH 8.6, and 2 mg/mL BSA). All unreacted MESNA was quenched with 100 mM iodoacetamide in PBS for 10 min before cells were lysed as described above. The steps following were the same as the protocol described above.

Fluorometry/BCECF Experiments. Cells were seeded on glass coverslips and grown until they reached 50−70% confluency. They were then placed in serum-free media for 5 h before transport was studied as described (*11*). In brief, control and test experiments were done on the same day using similarly acid selected cells of the same passage. Cells were seeded on glass coverslips, grown overnight in serum-free medium, and studied for transport. The cells were loaded with the acetoxymethyl ester of 2′7′-bis(carboxyethyl)5−6-carboxy-flouorescein (BCECF-AM, 5 μM) in Na^+ buffer (130 mM NaCl, 5 mM KCl, 2 mM $CaCl_2$, 1 mM $MgSO_4$, 1 mM NaH_2PO_4, 25 mM glucose, 20 mM HEPES, pH 7.4) for 30−60 min at room temperature, then washed with TMA buffer (130 mM tetramethylammonium chloride, 5 mM KCl, 2 mM $CaCl_2$, 1 mM $MgSO_4$, 1 mM NaH_2PO_4, 25 mM glucose, 20 mM HEPES, pH 7.4) to remove the extracellular dye, and the coverslip was mounted at an angle of 60° in a 100 μL fluorometer cuvette designed for perfusion and thermostated at 37 °C. The cells were pulsed with 40 mM NH_4Cl in TMA^+ buffer for 2−10 min, followed by removal of the NH_4Cl, and then the cells were perfused with TMA^+ buffer, which resulted in the acidification of the cells. In the wortmannin experiments, the cells were incubated with wortmannin (dissolved in DMSO) for 60 min while they were dye-loading.

Kinetic studies were performed as described (*11*) and did not include data from cells with an intracellular pH greater than pH 7.1, as there exists an endogenous acidification process in PS120 cells above this pH value. At pH_i values lower than pH 7.1, the pH recovery was entirely Na^+-dependent and amiloride-sensitive. Na^+/H^+ exchange rate data were calculated as the product of Na-dependent change in pH_i times the buffering capacity at each pH_i and were analyzed by a nonlinear regression data analysis program (Origin software), which allowed fitting of data to a general allosteric model described by the Hill equation, ($v = V_{max}[S]^n/(K' + [S]^n)$, with estimates for V_{max} and $K'[H^+]_i$ and their respective errors (SEM), as well as fitting to a hyperbolic curve, such as would be expected with Michaelis−Menten kinetics. The SEM was calculated by the computer to reflect variability of the parameters estimated.

RESULTS

PS120 Cells Target All Mature Glycosylated NHE1 to the Plasma Membrane While Only 14% of NHE3V in PS120 Cells Is Expressed on the Plasma Membrane. NHE-deficient PS120 fibroblasts were stably transfected with either NHE1 or NHE3 VSV-G-tagged at its C-terminus. The fraction of plasma membrane expression was determined as described under Experimental Procedures. Briefly, intact cells were surface biotinylated before being lysed, and biotinylated proteins were separated from unbiotinylated proteins by repeated avidin−agarose precipitations. The supernatant remaining after the avidin precipitations was verified to contain no remaining biotinylated proteins both by determining that no further biotinylated proteins precipitated with another round of avidin precipitation and by probing blots with HRP−streptavidin (data not shown). Three dilutions of the resulting fractions, total, surface, and intracellular, were resolved by SDS−PAGE and bands were visualized by ECL. The volume of individual bands was determined by use of a densitometer, and the volume of sample loaded was plotted against the density of individual bands. The fractions were compared against each other for the same densitometric value only when it fell in the linear range of the signals for all curves simultaneously.

The top panel of Figure 1A shows cell surface biotinylation results of two clones of NHE1V expressing different ratios of the 110 kDa mature glycosylated form to the 90 kDa immature form. The bottom panel is the corresponding

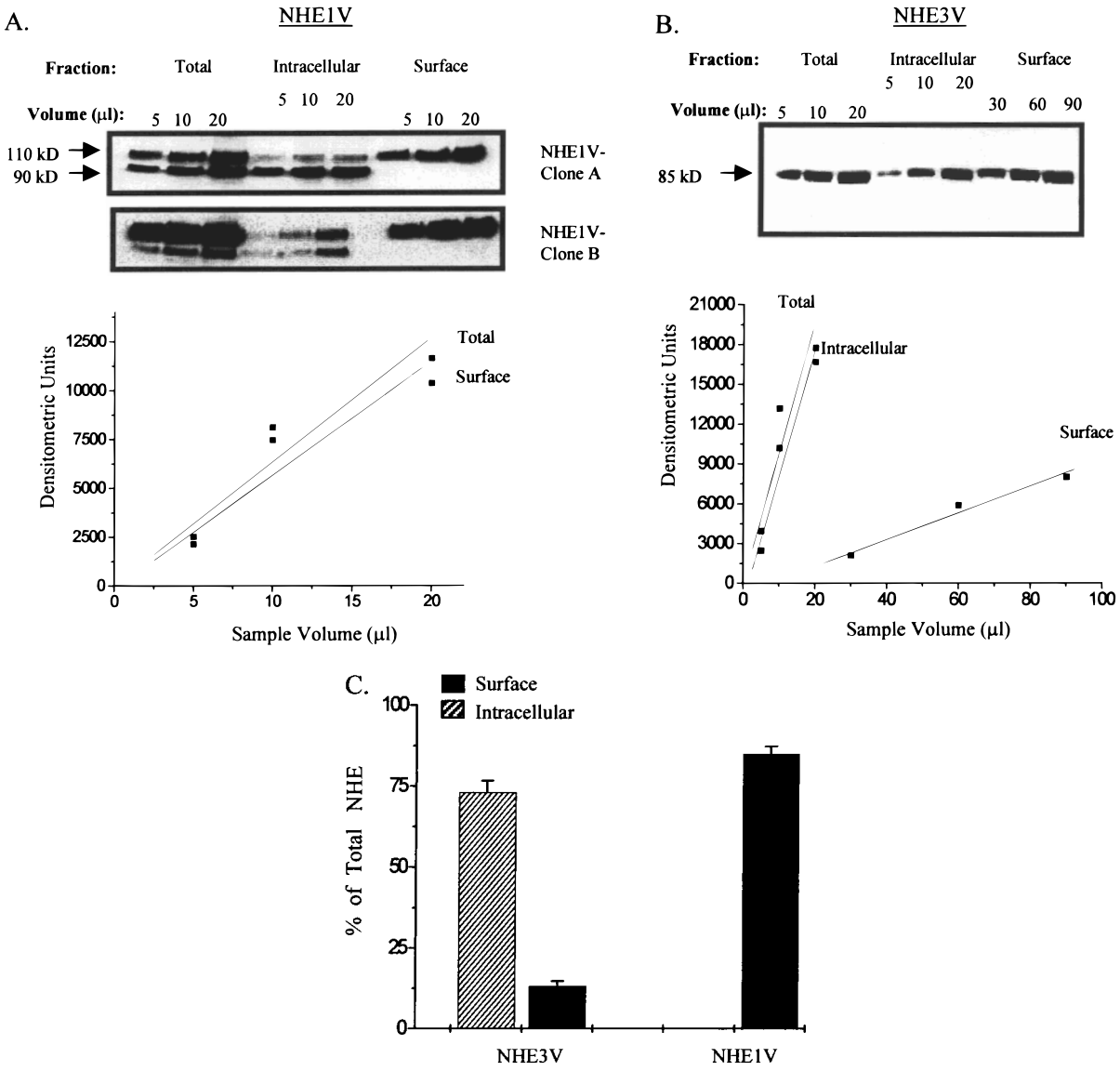

FIGURE 1: Cell surface biotinylation of NHE1V and NHE3V. Intact PS120 cells stably transfected with either NHE1V or NHE3V were serum-starved for ~5 h before being biotinylated as described under Experimental Procedures. (A) Western blots of two clones of NHE1V with three dilutions of total, intracellular, and surface fractions (top panel), probed with anti-VSV-G monoclonal antibody (P5D4) and visualized with ECL. Representative quantitation of 110-kDa NHE1V (clone B) (bottom panel) is also shown with density of bands determined by a scanning densitometer and Imagequant software and plotted against the sample volume. Fractions were compared for similar densitometric values across the overlapping linear range for all curves. At least three densitometric values were compared in the analysis of one Western blot. (B) Western blot of NHE3V with three dilutions of total, intracellular, and surface fractions (top panel), probed with anti-VSV-G monoclonal antibody (P5D4) and visualized with ECL. Representative quantitation (bottom panel) is also shown, with density of bands compared as discussed above. (C) Mean of surface (solid bars) and intracellular (hatched bars) fractions of NHE1V and NHE3V, shown ± SE. Experiments were repeated four times for each NHE1 clone. Experiments were repeated 10 times for NHE3V.

quantitation of the 110 kDa form of NHE1V clone B, with the percentage on the plasma membrane determined by comparing the volume of sample needed to give a similar densitometry value for all fractions present (total and surface). Intracellular levels of 110 kDa NHE1V were too low to quantitate. Both clones of NHE1V target nearly all (88% vs 85%) of their 110 kDa form to the plasma membrane, irrespective of the levels of total NHE1V expression or the relative amounts of the 110 and 90 kDa forms.

Cell surface biotinylation results for NHE3V are shown in Figure 1B. NHE3V is not glycosylated and appears as a single 85 kDa band with only 12% of exchangers present on the plasma membrane and 85% remaining within the cell. Again, as in the case of NHE1V, this subcellular distribution of NHE3V is consistently reproduced across multiple clones as well as mixed populations of stably expressing cells, demonstrating a wide variety of NHE3V expression levels (data not shown). A summary of the plasma membrane and intracellular fractions for NHE1V and NHE3V stably expressed in PS120 cells is shown in Figure 1C. NHE1V expresses 88.8% ± 3.5% of 110 kDa exchanger on the cell surface, while NHE3V expresses only 14.0% ± 1.3% of exchangers on the plasma membrane, with 83% ± 5.2% remaining within the cell.

Truncation of the C-Terminus of NHE3V Increases Basal Na^+/H^+ Exchange Activity and the Percentage of Exchanger on the Plasma Membrane. Since the plasma membrane fraction of NHE1V and NHE3V in PS120 cells was independent of expression level, appearing instead to be an

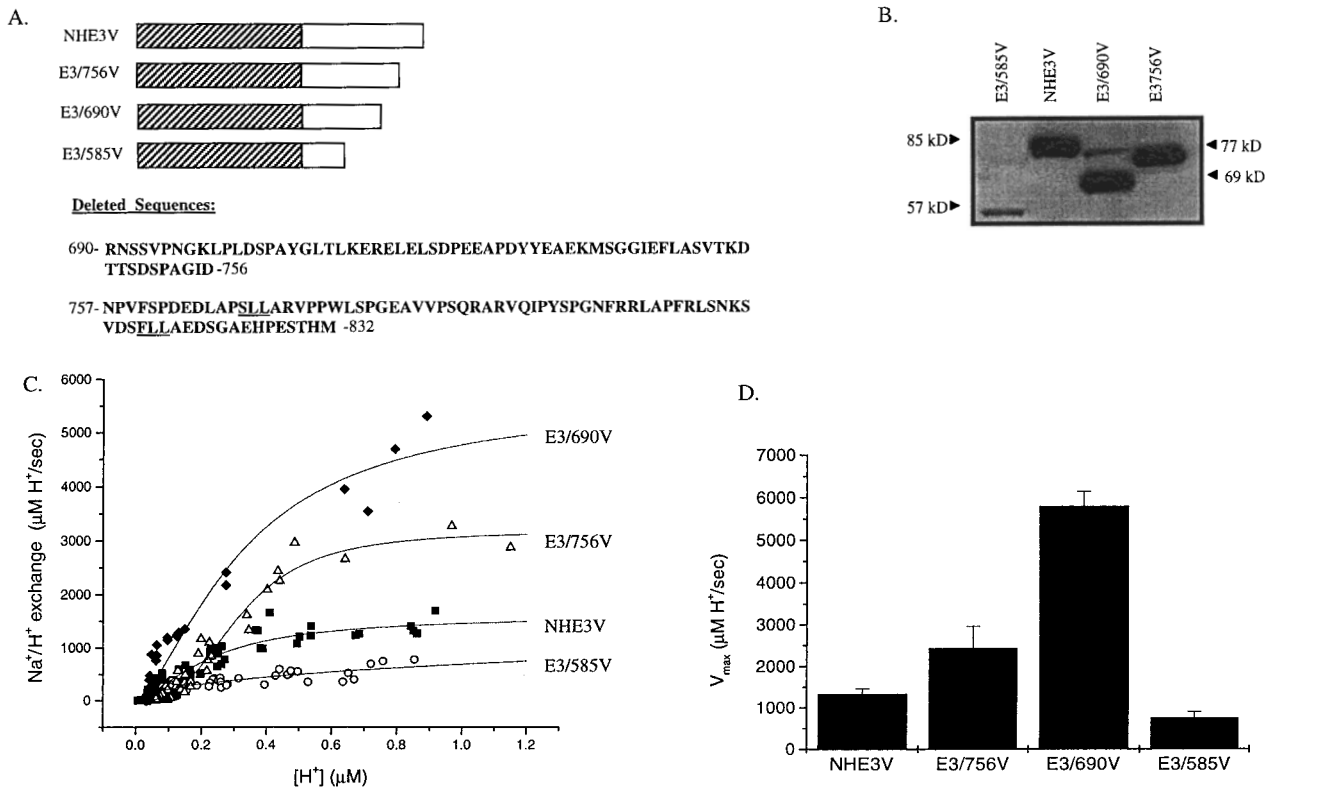

FIGURE 2: Expression and transport rates of NHE3V truncation mutants in PS120 cells. NHE3V truncation mutants were generated by PCR as described under Experimental Procedures. (A) The membrane-spanning domain of NHE3 is indicated as the *hatched bar* and the cytoplasmic domain as the *solid bar*. The amino acids deleted from NHE3V truncation mutants E3/690V and E3/756V are shown below with double leucine motifs underlined. (B) Western blot of equal amounts of total protein of cell lines stably expressing NHE3V, E3/756V, E3/690V, and E3/585V. (C) NHE3V (■), E3/756V (△), E3/690V(◆), and E3/585V (○) cells were loaded with BCECF in Na medium and then acidified by incubation with NH_4Cl, followed by perfusion in TMA^+ solution, and finally were allowed to recover to steady-state pH in Na^+ medium. The intracellular $[H^+]$ was monitored with BCECF in a spectrofluorometer. In these kinetic studies, H^+ efflux rates, equivalent to Na^+/H^+ exchange, were plotted against intracellular $[H^+]$. Na^+/H^+ efflux rates were calculated at various pH_i, lines were fit to the data by an allosteric model, and kinetic parameters [V_{max}, $K'(H^+)_i$, and n_{app}] were estimated. (D) Summary of basal V_{max} values for NHE3V and truncation mutants. Values were calculated from at least three full kinetic curves for each exchanger and shown as mean ± SE.

intrinsic characteristic of the particular protein, we hypothesized that the differences in this distribution could be attributed to a domain that is highly divergent between the two proteins, namely, the C-terminal cytoplasmic domain. Furthermore, we have previously shown that signaling pathways change the V_{max} of NHE3 through distinct C-terminal subdomains that work additively to determine both basal and regulated levels of Na^+/H^+ exchange activity (*11*). We therefore generated VSV-G-tagged C-terminal truncation mutants of NHE3, stably transfected them into PS120 cells, and studied them for total NHE expression levels, basal Na^+/H^+ exchange activity, and the percentage expressed on the plasma membrane. Figure 2A is a schematic of NHE3V indicating the sites used to generate the mutants as well as the amino acids deleted from E3/756V and E3/690V.

Figure 2B is a Western blot probed with anti-VSV-G of equal amounts of total protein (crude membrane preparations) from four mixed-population cell lines expressing full-length NHE3V or the truncation mutants, E3/756V, E3/690V, and E3/585V. We found that E3/756V and E3/690V expressed an equivalent amount of NHE protein as full-length NHE3V, but E3/585V demonstrated an 8-fold reduction in expression levels. Full kinetic curves were generated to determine the basal Na^+/H^+ exchange activity, with representative curves for all four cell lines shown in Figure 2C and summarized in Figure 2D. Full-length NHE3V had a V_{max} of 1300 ± 180 μM H^+/s. Removal of the C-terminal 76 amino acids (E3/756V) doubled the basal V_{max} to 2432 ± 530 μM H^+/s. Truncation of a further 66 amino acids (E3/690V) resulted in a further doubling of the basal V_{max} to 5794 ± 366 μM H^+/s. Finally, removal of another 105 amino acids (E3/585V) resulted in a much lower V_{max} of 750 ± 150 μM H^+/s. The $K'[H^+]_i$ values of full-length NHE3V and its truncation mutants remained unaltered at ~0.2 μM H^+ (data not shown).

To determine the mechanism for the altered basal V_{max} of the NHE3 truncation mutants, the percentage of NHE protein that each truncation mutant expressed on the plasma membrane was quantified by the cell surface biotinylation technique described above. E3/756V demonstrated a doubling of the percentage on the plasma membrane, increasing from 14% ± 1% for full-length NHE3V to 30% ± 1% for E3/756V. A representative Western blot and the corresponding quantitation of cell surface biotinylation for E3/756V are depicted in Figure 3A. Cell surface biotinylation results for E3/690V are shown in Figure 3B, demonstrating that removal of a further 66 amino acids increases the surface fraction to 55% ± 1% of total. Figure 3C shows cell surface biotinylation results for E3/585V, demonstrating that removal of another 105 amino acids does not increase the surface fraction, which remained essentially constant with 58% ± 6% of total NHE protein still on the plasma membrane. A summary of the plasma membrane fraction of NHE3V, E3/

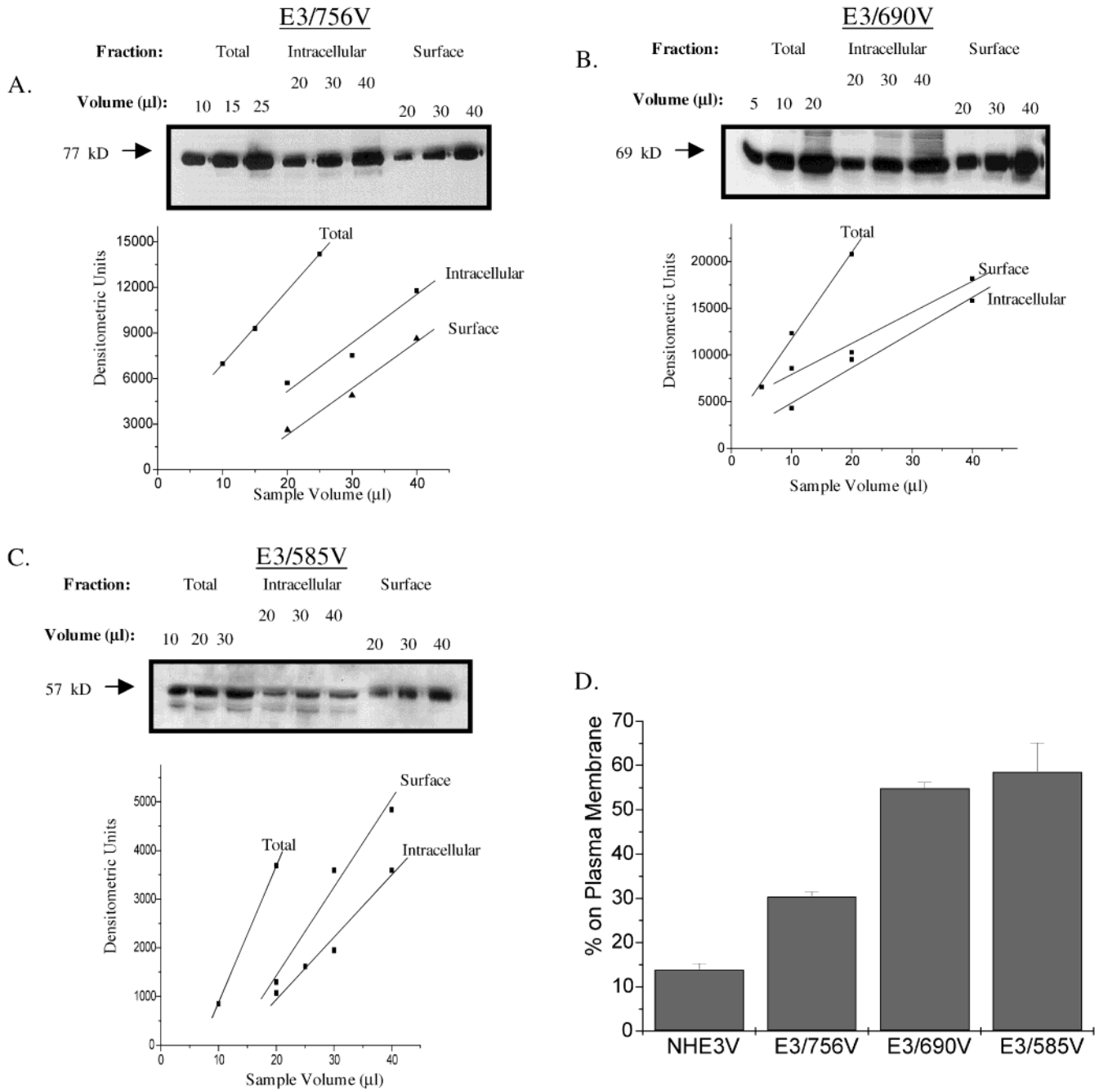

FIGURE 3: Surface levels of NHE3V truncation mutants. Intact PS120 cells stably expressing E3/756V, E3/690V, and E3/585V were serum-starved for ~5 h before being biotinylated as described above. Western blots of E3/756V (A), E3/690V (B), and E3/585V (C) with three dilutions of total, intracellular, and surface fractions (top panels) are shown. Representative quantitations are also shown (bottom panels) with density of bands compared as discussed above. (D) Summary of surface levels of NHE3V and truncation mutants. Experiments were repeated at least four times for each exchanger and are shown as mean ± SE.

756V, E3/690V, and E3/585V stably expressed in PS120 cells is shown in Figure 3D. The relative maximal activity of individual exchangers, calculated as the V_{max} per percentage of surface NHE (normalized for total expression levels), for full-length NHE3V and the truncation mutants E3/756V, E3/690V, and E3/585V are very similar, ranging from 108 to 120 μM H^+/% surface NHE. Therefore, it appears that the C-terminal 142 amino acids of NHE3V determines the fraction of surface NHE3V, without changing the maximal activity of individual exchangers. Truncation of a further 105 amino acids (E3/585V) fails to change levels on the plasma membrane or the maximal activity of individual exchangers. Since the domain mediating the fraction of plasma membrane expression for NHE3V was contained within the last 142 amino acids, all further studies were conducted with the full-length protein and two truncation mutants, E3/756V and E3/690V.

E3/756V and E3/690V Internalize Poorly Compared to Full-Length NHE3V. One possible explanation for the increased plasma membrane levels of E3/756V and E3/690V is an inability to internalize effectively, resulting in an accumulation on the cell surface. To test this possibility, we modified our cell surface biotinylation technique. Cells were surface biotinylated as before at 4 °C, they were then warmed to 37 °C for the indicated times, and finally cooled back down to 4 °C where all remaining surface biotin was stripped

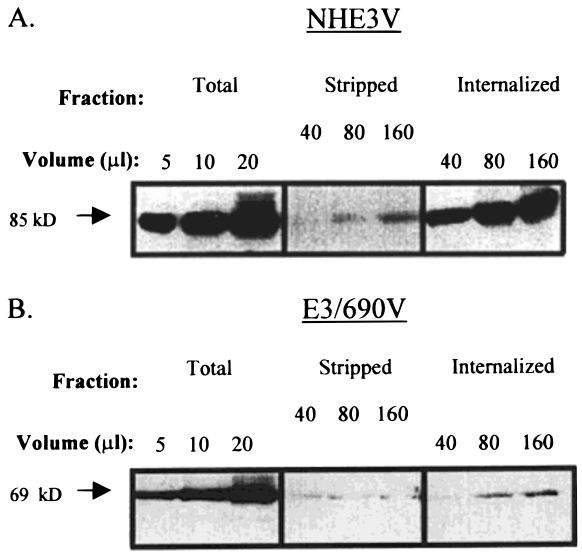

FIGURE 4: Internalization of NHE3V and E3/690V. Intact PS120 cells were serum-starved for ~5 h before being biotinylated at 4 °C as described above. Cells were then placed at 37 °C for 1 h before being returned to 4 °C, and surface biotin was stripped as described under Experimental Procedures. Results for NHE3V are shown in panel A and those for E3/690V are shown in panel B. Parallel plates were selected for equivalent amounts of total protein expressed (total), and one was stripped without a 37 °C incubation to check stripping efficiency (Stripped) while the other was allowed to internalize NHE3 protein for 1 h at 37 °C (internalized). Results are representative of four independent experiments.

before the cells were lysed and biotinylated proteins were precipitated with avidin−agarose. In this case, all remaining biotinylated proteins were protected from the stripping procedure because they were internalized during the 37 °C incubation period. Parallel plates were treated in three different ways: one was biotinylated as before to ensure the efficiency of the biotinylation reaction; one was stripped immediately following biotinylation without a 37 °C incubation to ensure that all surface biotin was effectively removed (stripped); the third was placed at 37 °C for 1 h before being stripped to determine the fraction of NHE protein internalized during the 1 h incubation (internalized). Reversible biotinylation results for NHE3V are shown in Figure 4A. Three dilutions of total, stripped surface, and internalized NHE3V were run on a Western blot, and the amount of internalized NHE3V was determined as the fraction of total. The high level of stripping efficiency was demonstrated by the absence of biotinylated proteins from the stripped fraction, while quantitation of the internalized fraction demonstrated that ~50% of surface NHE3V was endocytosed during the 1 h incubation period. In contrast, neither E3/756V nor E3/690V demonstrated any significant internalization during the 1 h incubation period, despite surface biotinylation occurring normally. Results for E3/690V are shown in Figure 4B, with similar results obtained for E3/756V (data not shown). This indicates that the increased plasma membrane levels of the NHE3 truncation mutants is at least partially due to their inability to endocytose, resulting in their elevated accumulation on the plasma membrane. The higher fraction of E3/690V on the plasma membrane (55%) compared to E3/756V (30%) would indicate that E3/690V internalizes less effectively than E3/756V despite neither one showing any appreciable internalization over the 1 h incubation. Therefore, longer internalization time points for E3/690V and E3/756V were studied. We found that neither truncation mutant internalizes during 1, 3, or 5 h incubation periods (data not shown). This could be explained by the internalization rates of E3/756V and E3/690V being significantly longer than 5 h and hence out of the range of detection of the above internalization assay.

PI3 Kinase Inhibition Reduces Na^+/H^+ Exchange and Surface Levels of NHE3V but Does Not Alter the Surface Levels or the Transport Activity of E3/756V or E3/690V. PI3 kinase has been implicated in mediating the exocytic portion of the recycling of NHE3V under basal conditions (*21*). Eliminating PI3 kinase activity by wortmannin treatment (100 nM, 37 °C) resulted in (1) a reduction of Na^+/H^+ exchange activity of NHE3V (Figure 5A), (2) reduced plasma membrane levels of NHE3V (Figure 5B), and (3) no change in the amount of internalized NHE3V, based on quantitation of internalized NHE3V in the presence of wortmannin using reversible biotinylation (data not shown). In contrast, wortmannin treatment did not alter the transport function, plasma membrane levels, or the internalization of E3/690V or E3/756V (Figure 5). The inability of wortmannin treatment to alter the transport rates or surface expression levels of E3/756V or E3/690V indicated that their higher plasma membrane levels were due entirely to poor endocytosis, because blocking recycling to the plasma membrane did not affect these mutants.

Two Double Leucine Motifs between Amino Acids 756−832 Are Not Involved in the Endocytosis of NHE3V. The truncation mutants of NHE3V have elevated surface levels because the exchanger is unable to endocytose effectively and consequently accumulates on the plasma membrane. The rapid internalization of NHE3V must be determined, therefore, by amino acids between 690 and 832. Double leucine residues have been shown to function as endocytic motifs for such membrane proteins as Glut4 (*22*), the interleukin 6 receptor (*23*), and the human immunodeficiency virus Nef protein (*22*, *24*). The domain between amino acids 756 and 832 for NHE3V contains two such motifs (indicated in Figure 2A), and we investigated their involvement in the internalization of the exchanger. The double leucines were deleted individually and together and transfected into PS120 cells. Cell surface biotinylation results for the double mutant (lacking both LL motifs) demonstrated that surface levels were not significantly different (12.7% ± 3.5% vs 14.0% ± 1.3%) from the wild-type NHE3V, indicating that these signals were not involved in the endocytosis of NHE3V. Similar results were obtained for both single mutants (data not shown).

Plasma Membrane Levels of NHE3V, E3/756V, and E3/690V Increase with Serum Treatment While Levels of NHE1V Remain Unaltered. The regulation of NHE3 in kidney cortex and Caco-2 cells in response to various agonists and antagonists such as phorbol esters (*13*), parathyroid hormone (PTH) (*15*), hypertension (*16*, *17*), and EGF has been linked to changes in plasma membrane NHE3. NHE3V, E3/756V, and E3/690V in PS120 cells all show stimulated Na^+/H^+ exchange rates in response to serum treatment (*11*). Consequently, we asked whether the serum stimulation of NHE3V could be mediated by changes in the membrane trafficking of the exchanger and whether the truncated NHE3V proteins retained the same mechanism for serum stimulation, despite having elevated basal surface levels. Cells were serum-

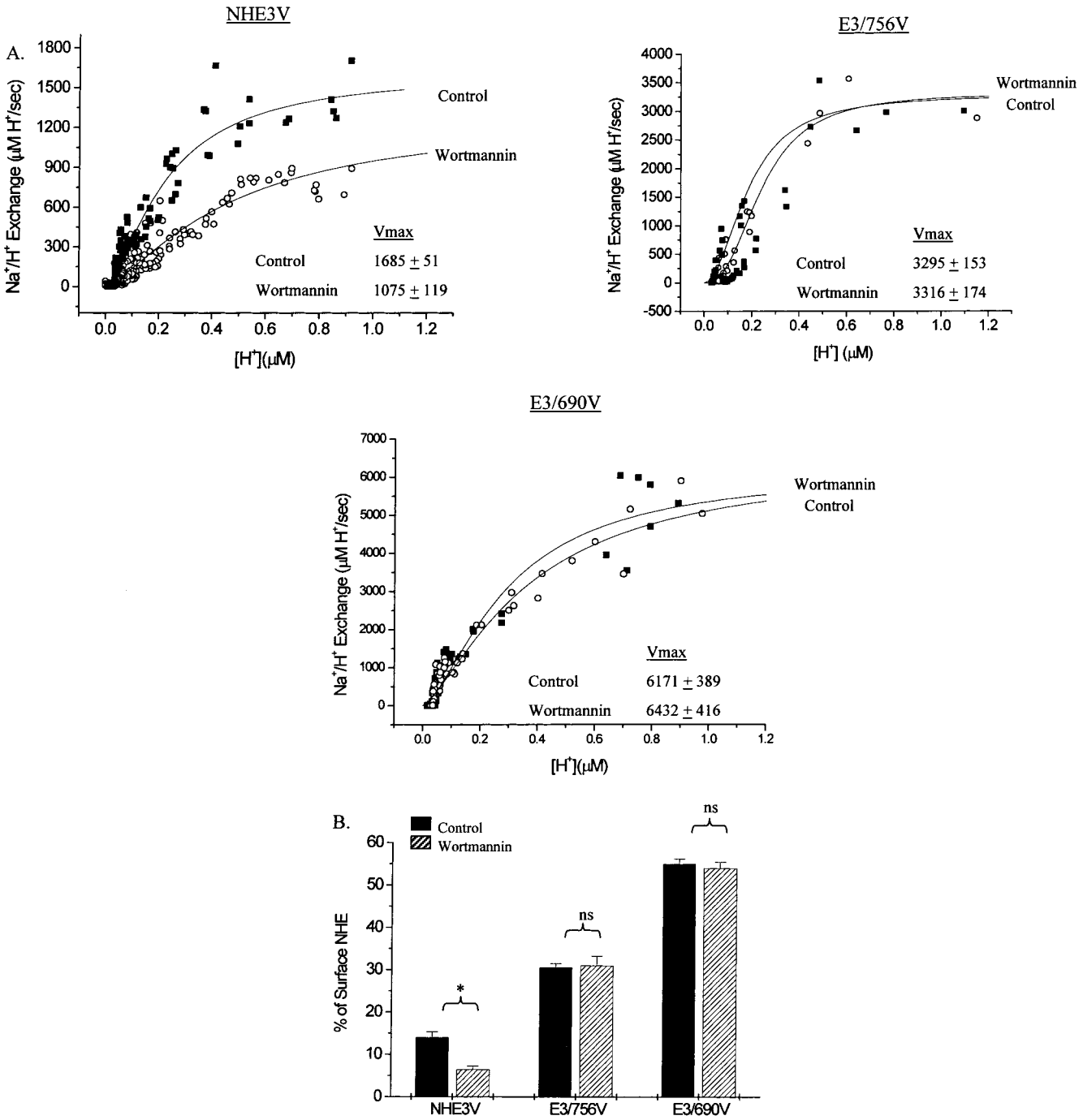

FIGURE 5: Wortmannin treatment of transport rates and surface levels of NHE3V, E3/756V, and E3/690V. (A) NHE3V, E3/756V, and E3/690V cells were loaded with BCECF in Na medium, alone or containing 100 nM wortmannin, for 1 h at 37 °C. The cells were then acidified by incubation with NH_4Cl, followed by perfusion in TMA^+ solution, and finally were allowed to recover to steady-state pH in Na^+ medium. The intracellular $[H^+]$ was monitored with BCECF in a spectrofluorometer and kinetic parameters were determined as described above. (B) Cells were serum-starved for ~5 h before being placed in fresh serum-free medium, alone or containing 100 nM wortmannin, for 1 h at 37 °C. They were then placed at 4 °C before being biotinylated, and surface fractions were determined as described above. Control surface levels are shown as solid bars and wortmannin surface levels as hatched bars. Experiments were repeated four times and shown as mean ± SE. Asterisk indicates $p = 0.001$; ns, not significant.

starved for ~5 h before being exposed to 10% fetal bovine serum (FBS) for 15 min at 37 °C and surface biotinylated, and the percentage on the plasma membrane was quantitated as described above. Figure 6 shows that NHE3V and its truncation mutants all show elevated plasma membrane levels with serum treatment. The plasma membrane levels of NHE3V increased from 14% to 22% of total, E3/756V surface levels increased from 30% to 43% of total, and E3/690V surface levels increased from 55% to 66% of total with serum treatment. In contrast, NHE1V surface levels remained the same. Therefore, the serum stimulation of NHE3V is at least partially attributable to an increase in the amount of active plasma membrane exchangers. This serum-mediated modulation of the membrane trafficking of NHE3V was retained in its truncation mutants, E3/756V and E3/690V, with all three showing a recruitment of ~10% of total NHE protein to the cell surface with serum treatment. Given the elevated basal surface levels of the NHE3V truncation

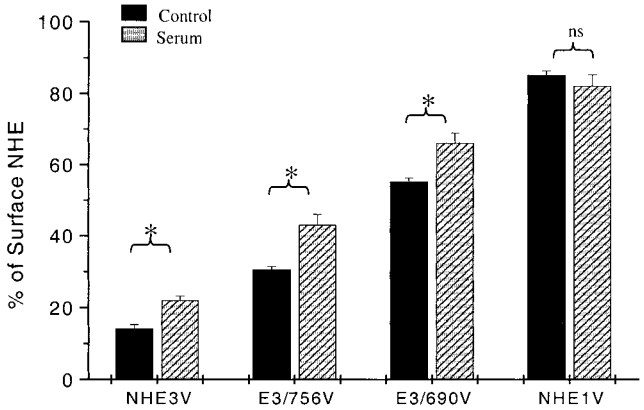

FIGURE 6: Acute serum treatment of NHE3V, E3/756V, E3/690V, E3/585V, and NHE1V. Cells were serum-starved for ~5 h before being placed in fresh serum-free medium, alone or containing 10% FBS, for 15 min at 37 °C. They were then placed at 4 °C before being biotinylated, and surface fractions were determined as described above. Control surface levels are shown as solid bars and serum levels as hatched bars. Experiments were repeated seven times and shown as mean ± SE. Asterisk indicates $p < 0.02$; ns, not significant.

mutants, the percent stimulation of serum was different between NHE3V, E3/756V, and E3/690V.

DISCUSSION

Biosynthetically mature NHE1 is found almost exclusively on the plasma membrane. In contrast, NHE3 is found both on the cell surface and within intracellular vesicles. Some of the intracellular NHE3 molecules are derived from the redistribution of the exchanger from the plasma membrane, as a part of the basal recycling of the protein. Changes in the rapid recycling of NHE3 provide a means to regulate the percentage of exchanger at the surface membrane and thus regulate total Na^+/H^+ exchange activity. Previous studies have examined the basal recycling of NHE3 (*19*, *21*) as well as changes in this recycling under a variety of regulatory conditions (*13*, *16*, *17*). What have not been identified are determinants within NHE3 that are involved in either the basal or regulated movement of the protein to and from the cell surface. In this study, we have developed a method of cell surface biotinylation that allowed the quantitation of the percentage of plasma membrane molecules as a fraction of the total. Analysis of C-terminal truncation mutants of NHE3 using this method allowed the identification of two adjacent domains in the C-terminus of the exchanger, which determine the levels of basal Na^+/H^+ exchange by regulating the endocytosis of NHE3. In contrast, neither of these domains affected the increase in plasma membrane NHE3 caused by acute serum treatment. In the NHE3 truncation mutants, which endocytose extremely poorly, the intact serum regulation indicated a stimulation of exocytosis, demonstrating that different parts of the NHE3 C-terminus are involved in controlling plasma membrane expression under basal and serum-stimulated conditions.

The use of impermeant biotin analogues to label membrane proteins is a widely used technique to examine cell surface expression. Here, we report quantitative analysis with this technique that allows the determination of the percentage of NHE protein on the plasma membrane. Reported methodological issues that affect quantitative interpretations of biotinylation data have included concerns about the efficiency of the modification as well as possible contamination of intracellular pools (*25*). Our biotinylation results for NHE1V addresses both these issues. To independently confirm our results, we used previous studies of the percentage of NHE1 on the plasma membrane (*26*). Extracellular chymotryptic cleavage of NHE1 demonstrated that all the mature glycosylated protein was susceptible to degradation and hence was localized to the cell surface, while the smaller biosynthetic intermediate was protected from cleavage and consequently must be localized intracellularly. Consistent with these results, we found that 88% of mature NHE1 was retrieved through avidin precipitations, indicating that essentially all surface NHE1 was modified by incubation with biotin. Furthermore, none of the smaller form of NHE1 was detected in the surface fractions, demonstrating that intracellular proteins were not being labeled. The similar results obtained for the plasma membrane expression of NHE1 using either extracellular chymotryptic cleavage or cell surface biotinylation validated this use of quantitative biotinylation. In addition, the similar membrane topology of all NHEs and the conserved presence of extracellular lysine residues suggested that the biotinylation results for NHE1 could be extrapolated to other NHE isoforms.

Cell surface biotinylation results indicated that, unlike the plasma membrane expression of NHE1V, only 14% of NHE3V was found on the cell surface. The characteristic surface expression patterns of both NHE isoforms were consistently reproduced across a wide variety of expression levels and remained unaltered among clones expressing equivalent levels of NHE1V and NHE3V. These results suggested that the differences in subcellular distribution between the two NHE isoforms were attributes of NHE1 vs NHE3 and not simple products of overexpression. In fact, the polarized epithelial cells of the intestine and kidney proximal tubule, which express both NHE1 and NHE3, share the same pattern of plasma membrane targeting as demonstrated in PS120 fibroblasts. Namely, all the mature NHE1 is targeting to the basolateral membrane, while NHE3 is found both on the brush border membrane and in subapical vesicles, although a higher percent of total NHE3 is present on the apical surface than on the plasma membrane of fibroblasts.

The low surface fraction of NHE3V is consistent with the rapid recycling of the protein from the cell surface to juxtanuclear recycling endosomes. To identify determinants in the basal recycling of NHE3V, we examined the cell surface expression of several C-terminal truncation mutants of NHE3V. This was done not only because the C-terminus of NHE3 is extremely divergent from that of NHE1 but also because our previous studies have demonstrated elevated basal NHE3 activity with the truncation of the C-terminal 76 amino acids. However, it had not been elucidated whether this stimulation was caused by a change in the amount of plasma membrane NHE3 or was due to changes in the NHE3 transport activity.

Our present results indicate that the stimulation of Na^+/H^+ exchange was due entirely to the presence of more surface NHE3 molecules and suggests that the C-terminal 142 amino acids of NHE3 act to inhibit plasma membrane NHE3 expression under basal conditions. In addition, these results led to the surprising conclusion that removal of the

majority of the regulatory domain of NHE3 (277 of the 377 amino acids that comprise the cytoplasmic domain) did not alter the basal activity of individual NHE3 molecules. Furthermore, our results suggest that the plasma membrane expression level of NHE3 is regulated in at least two steps. Removal of the C-terminal 76 amino acids resulted in the loss of at least one of these putative signals, with surface levels doubling from 14% to 30% of total NHE3V now on the plasma membrane. Truncation of another 66 amino acids removed the other putative signal with surface levels rising to 55% of total, which was unaltered with the removal of a further 105 amino acids. The plasma membrane fractions of the NHE3V truncation mutants were consistently reproduced across multiple expression levels, indicating that total protein levels were not determining the extent of surface expression. Rather, these specific domains influenced the surface expression of NHE3.

The stepwise increase in surface fraction with the NHE3 truncation mutants implies the presence of multiple signals controlling how much exchanger is localized to the plasma membrane. Given the large stretches of amino acids truncated in the mutants, we favor the presence of two or more distinct signals vs one large domain contained within the C-terminal 142 amino acids, the effect of which is partially abrogated with the removal of the C-terminal 76 amino acids.

Given that NHE3 recycles under basal conditions, alterations in the rates of endocytosis or exocytosis could potentially have been responsible for changing the amount of basal plasma membrane NHE3. The rapid basal recycling of NHE3V was examined in two ways. First, reversible cell surface biotinylation demonstrated that ~50% of surface NHE3V was internalized during a 1 h incubation at 37 °C. In contrast, the NHE3V truncation mutants demonstrate no appreciable internalization for up to 5 h. Second, previous studies have demonstrated that the exocytosis of NHE3V from recycling endosomes is mediated by the lipid kinase, PI3 kinase. These studies also established a specific role for PI3 kinase in its regulation of NHE3 movement. Unlike other reported observations of the role of PI3 kinase in the membrane trafficking of other plasma membrane proteins as well as in bulk membrane movement, PI3 kinase worked almost exclusively in mediating the exocytosis of NHE3 (*21*). Accordingly, the inhibition of PI3 kinase with wortmannin for 1 h decreased NHE3V transport rates and surface levels by ~50% without altering the amount of internalized NHE3V. In contrast, the inhibition of PI3 kinase failed to affect either transport rates or plasma membrane fractions of the truncation mutants. Both the inability to internalize effectively and the lack of effect with the block of exocytosis are consistent with a model of the truncated NHE3V proteins lacking the domains mediating the basal endocytosis of the exchanger and hence accumulating on the cell surface.

Since truncated NHE3V internalized poorly, we hypothesized that endocytic motifs within the C-terminal 142 amino acids of the protein were mediating the internalization of the exchanger. Motifs that have previously been shown to be involved in endocytosis and that are present within the C-terminal 142 amino acids of NHE3 include two double leucine motifs. These motifs have been shown to be involved in the endocytosis of Glut4 (*22*) and the interleukin 6 receptor (*23*). However, mutations of these two double leucine motifs either alone or together failed to alter the basal NHE3 exchange rate or the percentage of NHE3 on the plasma membrane. While no other recognized endocytic motifs are located within the C-terminal 142 amino acids, we postulate the presence of either unrecognized endocytic motifs or the involvement of NHE3-associated proteins that mediate the basal endocytosis of NHE3. In fact, we have reported that calmodulin binds within the last 76 amino acids of NHE3 and the abrogation of this binding results in a stimulation of NHE3 activity. Whether the binding of calmodulin to NHE3 influences the membrane trafficking of the exchanger remains to be defined (*27*).

The rates of recycling of NHE3V are altered by a variety of signaling pathways, which culminate in a change in the number of exchangers on the plasma membrane. Acute serum treatment has been shown to stimulate the Na^+/H^+ exchange of NHE3V and appears to act through the very N-terminal portion of the C-terminus of the protein (*11*). Cell surface biotinylation showed that the serum-mediated increase in NHE3V activity was at least partially attributable to an increase in plasma membrane exchangers. Furthermore, the mechanism of serum stimulation (i.e., movement of molecules to the cell surface) was retained between full-length NHE3V and its truncation mutants, which all mobilized ~10% of total NHE3 molecules to plasma membrane within 15 min of serum exposure. The ability of the NHE3V truncation mutants to be mobilized to the cell surface with serum stimulation demonstrated that NHE3V trafficked differently under basal and regulated conditions, with distinct modulators of both processes found within the protein.

Membrane trafficking has been implicated in the regulation of numerous transport proteins, including the vasopressin-mediated exocytosis of aquaporin 2 (*28*) and the parathyroid hormone-mediated endocytosis of NaPi-2 (*29*). In contrast, the trafficking of NHE3 appears to play a role not only in changing plasma membrane levels of the exchanger under specific regulatory conditions but also in determining the basal surface levels of NHE3. Our results suggest that, under basal conditions, NHE3 is rapidly endocytosed from the plasma membrane through determinants localized to the C-terminal 142 amino acids. This implies NHE3 exists in an "inhibited" condition, with internal signals limiting the extent of plasma membrane expression of the exchanger. The rapid basal recycling of NHE3, mediated potentially through multiple motifs, allows signaling pathways to change NHE3 activity by altering how the exchanger is endocytosed or exocytosed.

REFERENCES

1. Wakabayashi, S., Shigekawa, M., and Pouyssegur, J. (1997) *Physiol. Rev. 77*, 51−74.
2. Orlowski, J., and Grinstein, S. (1997) *J. Biol. Chem. 272*, 22373−22376.
3. Rotin, D., and Grinstein, S. (1989) *Am. J. Physiol. 257*, C1158−C1165.
4. Tominaga, T., and Barber, D. L. (1987) *Mol. Biol. Cell 9*, 2287−2303.
5. Grinstein, S., Woodside, M., Waddell, T. K., Downey, G. P., Orlowski, J., Pouyssegur, J., Wong, D. C., and Foskett, J. K. (1993) *EMBO J. 12*, 5209−5218.
6. Counillon, L., Pouyssegur, J., and Reithmeier, R. A. (1994) *Biochemistry 33*, 10463−10469.
7. Helmle-Kolb, C., Counillon, L., Roux, D., Pouyssegur, J., Mrkic, B., and Murer, H. (1993) *Pflugers Arch. 425*, 34−40.

8. Wakabayashi, S., Bertrand, B., Shigekawa, M., Fafournoux, P., and Pouyssegur, J. (1994) *J. Biol. Chem. 269*, 5583−5588.
9. Bianchini, L., and Pouyssegur, J. (1996) *Kidney Int. 49*, 1038−1041.
10. Coupaye-Gerard, B., Bookstein, C., Duncan, P., Chen, X. Y., Smith, P. R., Musch, M., Ernst, S. A., Chang, E. B., and Kleyman, T. R. (1996) *Am. J. Physiol. 271*, C1639−C1645.
11. Levine, S. A., Nath, S. K., Yun, C. H., Yip, J. W., Montrose, M., Donowitz, M., and Tse, C. M. (1995) *J. Biol. Chem. 270*, 13716−13725.
12. Biemesderfer, D., Rutherford, P. A., Nagy, T., Pizzonia, J. H., Abu-Alfa, A. K., and Aronson, P. S. (1997) *Am. J. Physiol. 273*, F289−299.
13. Janecki, A. J., Montrose, M. H., Zimniak, P., Zweibaum, A., Tse, C. M., Khurana, S., and Donowitz, M. (1998) *J. Biol. Chem. 273*, 8790−8798.
14. Peng, Y., Preisig, P. A., Amemiya, M., Moe, O. W., Yanagisawa, M., and Alpern, R. J. (1998) *J. Am. Soc. Nephrol. 9*, A0051 (abstract).
15. Callazo, R., Fan, L., Wiederkehr, M., Zhao, H., Crowder, L., and Moe, O. W. (1998) *J. Am. Soc. Nephrol. 9*, A0018 (abstract).
16. Yip, K. P., Tse, C. M., McDonough, A. A., and Marsh, D. J. (1998) *Am. J. Physiol. 275*, F565−F575.
17. Zhang, Y., Magyar, C. E., Norian, J. M., Holstein-Rathlou, N. H., Mircheff, A. K., and McDonough, A. A. (1987) *Am. J. Physiol. 274*, C1090−C1100.
18. Akhter, S., Cavet, M., Tse, C. M., and Donowitz, M. (1997) *Gastroenterology 114*, A347, G1415 (abstract).
19. D'Souza, S., Garcia-Cabado, A., Yu, F., Teter, K., Lukacs, G., Skorecki, K., Moore, H. P., Orlowski, J., and Grinstein, S. (1987) *J. Biol. Chem. 273*, 2035−2043.
20. Levine, S. A., Montrose, M. H., Tse, C. M., and Donowitz, M. (1993) *J. Biol. Chem. 268*, 25527−25535.
21. Kurashima, K., Szabo, E. Z., Lukacs, G., Orlowski, J., and Grinstein, S. (1998) *J. Biol. Chem. 273*, 20828−20836.
22. Corvera, S., Chawla, A., Chakrabarti, R., Joly, M., Buxton, J., and Czech, M. P. (1994) *J. Cell Biol. 126*, 1625.
23. Dittrich, E., Haft, C. R., Muys, L., Heinrich, P. C., and Graeve, L. (1996) *J. Biol. Chem. 271*, 5487−5494.
24. Craig, H. M., Pandori, M. W., and Guatelli, J. C. (1998) *Proc. Natl. Acad. Sci. U.S.A. 95*, 11229−11234.
25. Gottardi, C. J., Dunbar, L. A., and Caplan, M. J. (1995) *Am. J. Physiol. 268*, F285−F295.
26. Shrode, L. D., Gan, B. S., D'Souza, S. J., Orlowski, J., and Grinstein, S. (1998) *Am. J. Physiol. 275*, C431−C439.
27. Donowitz, M., Kambadur R, Zizak, M., Nath, S., Akhter, S., and Tse, C. M. (1997) *Gastroenterology* A360 (abstract).
28. Knepper, M. A., and Inoue, T. (1997) *Curr. Opin. Cell Biol. 9*, 560−564.
29. Murer, H., and Biber, J. (1996) *Exp. Nephrol. 4*, 201−204.

BI991739S